

# IoT-Based Thermal Comfort Monitoring System in High-Temperature Workspaces

Johansen C. Mandey, Alvin J. Tinangon, Rachmat Prijadi

Department of Architecture Engineering, Sam Ratulangi University, Manado, Indonesia

Email: [johansen.mandey@unsrat.ac.id](mailto:johansen.mandey@unsrat.ac.id)

Received: 23 November 2025; revised: 15 January 2025; accepted: 18 February 2026

## Abstract

High-temperature work environments pose significant challenges to occupational safety and thermal comfort monitoring. This study presents the design and functional validation of an Internet of Things (IoT)-based thermal microclimate monitoring system intended for high-temperature indoor workspaces. The proposed system integrates multiple microclimate sensors with an ESP32-based platform to acquire temperature, humidity, air velocity, and globe temperature data. Sensor data are transmitted wirelessly to a cloud server for real-time visualization and computation of thermal comfort indices, including Predicted Mean Vote (PMV) and Wet Bulb Globe Temperature (WBGT). Prototype validation results demonstrate stable sensor operation and reliable real-time data transmission to the cloud platform. The system is shown to be feasible as a prototype solution for supporting thermal environment monitoring and occupational safety assessment in tropical climates. Future work will focus on full-scale field deployment, long-term performance evaluation, and integration of predictive control strategies for automated ventilation systems.

Keywords— IoT, microclimate sensor, thermal comfort, PMV, WBGT.

## I. INTRODUCTION

Thermal comfort is a critical factor influencing worker performance, safety, and well-being in high-temperature workplaces. Exposure to elevated temperature, humidity, and radiant heat can impair concentration, reduce productivity, and increase the risk of heat-related illnesses such as heat exhaustion and heat stroke [1], [2]. Thermal comfort itself represents a heat balance between the human body and its surrounding environment, and is shaped by key environmental parameters such as air temperature, humidity, and air velocity, as well as personal factors including clothing insulation and physical activity level [3]. Commercial kitchens present an even more challenging thermal environment, as continuous cooking activities generate substantial sensible and latent heat that elevates air temperature, humidity, and radiant heat levels. Previous studies have reported that kitchens are among the largest contributors to thermal discomfort due to heat accumulation during cooking activities. Their field measurements further showed that kitchen temperatures fluctuate considerably during morning and evening cooking hours and often fall within “warm” thermal sensation

category. Ventilation conditions also play a critical role, where inadequate openings or heat-trapping ceiling structures result in higher indoor temperatures compared to kitchens with better airflow. Despite the importance of this issue, research specifically focusing on thermal comfort in non-air-conditioned kitchen environments remains limited. Rahmillah et al. highlight that only “relatively few studies on thermal comfort in kitchen” have been conducted, with most thermal comfort research centered on seasonal climates rather than tropical settings. This gap underscores the need for updated assessments using continuous monitoring technologies suited to environments characterized by high internal heat loads and variable ventilation patterns. [3]

Moreover, in tropical and middle-income countries, the risk of occupational heat exposure is intensified by high ambient temperatures, heavy physical workloads, and limited access to effective cooling mechanisms. [4].

In commercial kitchens, heat exposure becomes even more complex. Sensible and latent heat emitted from stoves, ovens, and other cooking appliances can substantially raise air temperature and radiant heat levels, creating a heavy microclimate burden. A study of kitchen workers in Ethiopia reported a high prevalence of heat-related symptoms—including dizziness, heavy sweating, and fatigue—strongly associated with elevated Wet Bulb Globe Temperature (WBGT) values within the workspace [1]. Similar findings in other industrial kitchen settings show that inadequate ventilation and intense radiant heat from cooking equipment intensify thermal loads on workers, reinforcing the need for systematic microclimate management [5].

WBGT has become one of the most widely used indicators for assessing occupational heat stress because it accounts for air temperature, humidity, radiant heat, and air movement. Recent literature emphasizes that WBGT outperforms alternative indices—such as the Heat Index—when evaluating heat stress in physically demanding work environments [6]. In many tropical and developing regions, WBGT thresholds are frequently exceeded, highlighting the need for adaptive strategies and continuous monitoring to protect workers from heat-related health risks [7].

Beyond health impacts, heat stress has been shown to significantly reduce productivity. Meta-analyses in construction and industrial workforces indicate a notable decline in work output when WBGT surpasses certain critical limits. These findings underscore the importance of monitoring microclimate conditions in real time to support timely interventions [8].

In tropical climates, kitchens and other high-temperature workspaces pose a particular challenge due to high ambient temperatures, humidity and heat sources from cooking equipment. Traditional thermal comfort assessment often relies on spot measurements or manual logging, which limits temporal resolution and prevents real-time intervention. The Internet of Things (IoT) enables distributed sensing, networked data collection, and cloud-based analytics, providing an opportunity to monitor microclimate parameters continuously.

This study focuses on the design, implementation, and validation of an IoT-based thermal microclimate monitoring system, rather than on establishing new baseline thermal comfort conditions. Field measurements previously reported using calibrated industrial instruments were used solely as reference data for sensor calibration and system verification, not as the primary data source for analysis.

All real-time data presented in this study are acquired through the developed IoT system installed at the study site. Synthetic or representative data series are used only for illustrating visualization capability and system behavior, and are explicitly labeled as such. The objectives are to (1) design an IoT sensor network for microclimate monitoring, (2) validate PMV and WBGT computations against field measurements, and (3) demonstrate the utility of real-time monitoring for occupational safety and energy-aware ventilation strategies.

Traditional thermal comfort assessments frequently rely on the Predicted Mean Vote (PMV) and Predicted Percentage of Dissatisfied (PPD) indices. In their study, Rahmillah et al. reported PMV values ranging from 1.73 to 2.36, indicating “warm” sensations with PPD values between 63% and 90% [3]. They also note that PMV/PPD may not be fully appropriate for commercial kitchens with high metabolic workloads and intense heat sources, as these conditions fall outside standard PMV assumptions (p. 6). This limitation highlights the need for complementary indices such as the Wet Bulb Globe Temperature (WBGT), which incorporates humidity, radiant heat, and air movement for more accurate assessment of occupational heat stress.

Predicted Mean Vote (PMV) and Predicted Percentage of Dissatisfied (PPD) were developed by Fanger and are standardized in ISO 7730. PMV predicts the mean thermal sensation vote of a large group on a scale from -3 (cold) to +3 (hot). PMV is a function of air temperature, radiant temperature, air velocity, humidity, clothing insulation and metabolic rate[9]. The PPD is derived from PMV to estimate the fraction of people dissatisfied. Wet Bulb Globe Temperature (WBGT) is an index used to assess heat stress, combining wet bulb (humidity influence), globe (radiant heat

and air temperature in weighted form (ISO 7243). Several studies have applied PMV and WBGT for evaluating thermal comfort in workplaces and industry [10], [11]. Recent work has focused on IoT-enabled thermal monitoring and integration with building management systems to facilitate adaptive ventilation and energy savings [12],[13],[14],[15].

The PMV can be computed using the energy balance of the human body. A commonly used equation (1) is:

$$PMV = (0.303 * \exp(-0.036 * M) + 0.028) * L \quad (1)$$

where M is the metabolic rate ( $W/m^2$ ) and L is the thermal load on the body ( $W/m^2$ ). Detailed computation follows ISO 7730.

Advances in Internet of Things (IoT) technologies now enable continuous high-resolution monitoring of environmental parameters such as air temperature, relative humidity, air velocity, and radiant heat using globe temperature sensors. Such systems are essential for identifying microclimate “hot spots,” detecting rapid thermal fluctuations during cooking activities, and providing early warnings of dangerous heat exposure. IoT-based monitoring also supports more adaptive ventilation control and operational decision-making.

In tropical regions such as Indonesia, where high humidity compounds the effects of heat exposure, real-time microclimate monitoring systems have substantial potential to enhance thermal comfort and reduce occupational heat-stress risks. Motivated by these challenges, this study develops and evaluates an IoT-based microclimate monitoring system capable of continuously measuring key environmental parameters in commercial kitchen settings. The system computes WBGT in real time and visualizes data through an integrated dashboard to support managerial and operational decisions related to ventilation, cooling, and worker safety.

## I. METHODOLOGY

### A. System Architecture

The proposed IoT system comprises distributed microclimate sensor nodes, a microcontroller gateway, a cloud platform for data storage and visualization, and a user dashboard. Each sensor node measures air temperature, relative humidity, globe temperature (as proxy for mean radiant temperature), and air velocity. An ESP32 microcontroller is used as the core node controller for local data aggregation and Wi-Fi transmission. The cloud platform computes PMV and WBGT indices in real-time and stores time-series data for later analysis. Figure 1 illustrates the system block diagram.

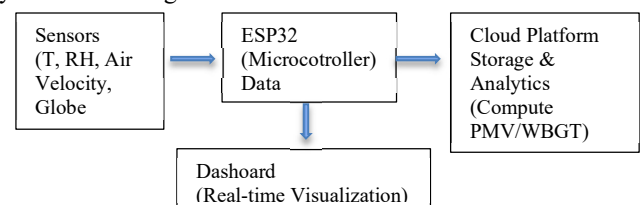


Figure 1. IoT system block diagram (sensor nodes → ESP32 gateway → Cloud platform → Dashboard).

The thermal microclimate monitoring system developed in this study is implemented as an Internet of Things (IoT) platform consisting of three functional layers: (1) the sensing layer, (2) the communication layer, and (3) the cloud processing and visualization layer. This design ensures that all environmental data are transmitted in real time through the internet and stored on a remote server for continuous monitoring and analysis (see figure 2).

1) Sensing Layer (Sensor Node)

The sensing layer consists of an ESP32-based microcontroller connected to multiple environmental sensors, including: Temperature and humidity sensor (DHT22/SHT31), Air velocity sensor, Globe temperature sensor, Additional microclimate sensors if required. The ESP32 collects all measurements at predefined intervals (e.g., every 5–10 seconds), packages them into JSON-formatted payloads, and prepares them for wireless transmission.

2) Communication Layer (Wireless IoT Transmission)

To ensure that data are delivered as an IoT stream, the ESP32 communicates with the cloud server using WiFi-based MQTT (Message Queuing Telemetry Transport) — a lightweight IoT protocol widely used for real-time sensor networks. MQTT Transmission Workflow: (1) The sensor node connects to a local WiFi access point. (2) The ESP32 publishes data to an MQTT broker using a unique topic, for example: `iot/kitchen/thermal/data`. (3) Each data packet contains: `{ "temperature": 31.5, "humidity": 76.2, "globe_temp": 34.1, "air_velocity": 0.21, "timestamp": "2024-12-15T14:32:05" }`

(4) The MQTT broker forwards the data to the cloud processing layer. The use of MQTT confirms that the system is not merely data logging locally but truly transmitting data through an IoT protocol.

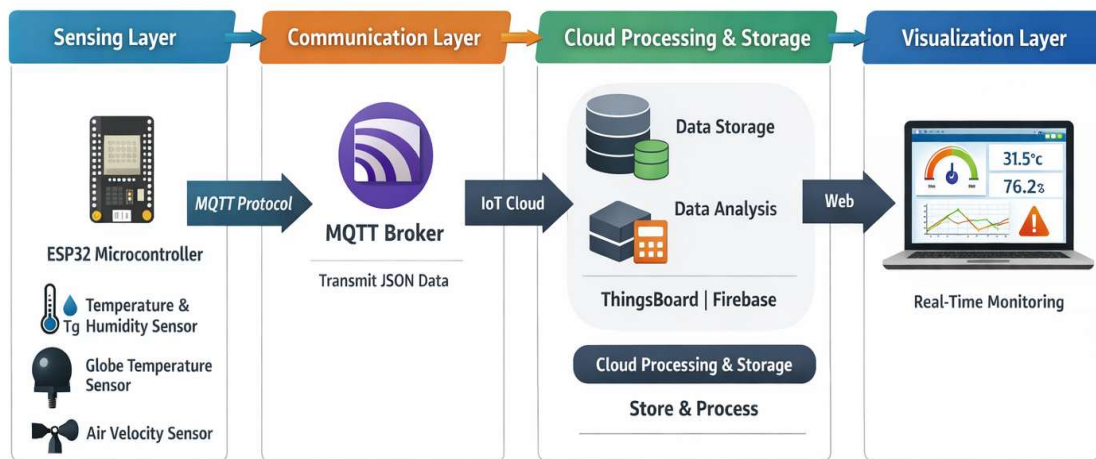


Figure 2. IoT thermal microclimate monitoring system

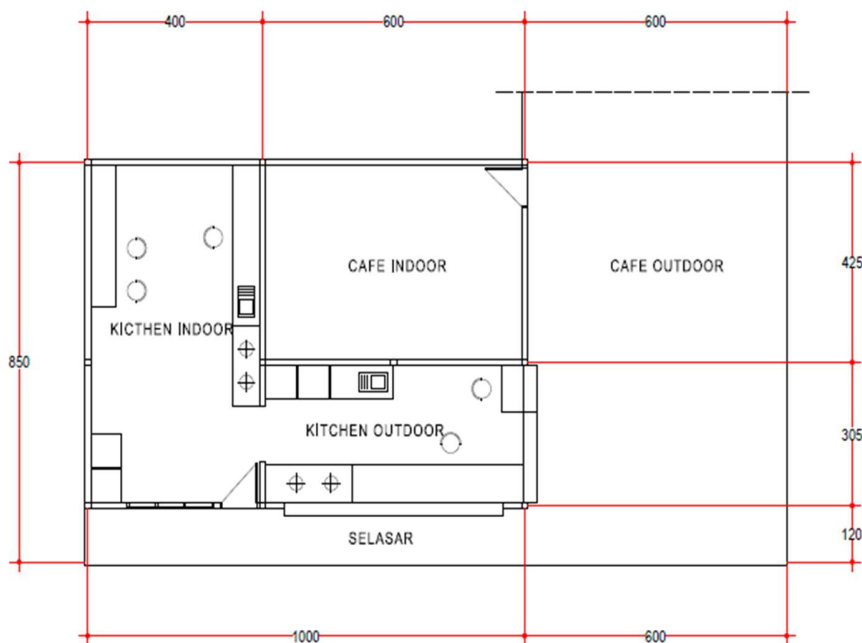


Figure 3. Indoor and Outdoor Kitchen Plans

### 1) Cloud Processing and Storage Layer

A cloud IoT platform (such as ThingsBoard, Thingspeak, Firebase Realtime Database, or a custom server) receives all MQTT messages, stores them, and makes them available for historical and real-time analysis. Cloud Functions Include: Receiving MQTT payloads, Parsing sensor data, Storing values in a cloud database, Computing derived indices (e.g., PMV or WBGT), Synchronizing data for dashboards and reports. This cloud integration is essential evidence that the system is IoT-based.

### 2) Visualization Layer (Dashboard and Analytics)

A real-time dashboard was developed to visualize environmental data streamed from the cloud server. The dashboard displays: Real-time temperature, humidity, air velocity, globe temperature, Time-series graphs with live updates, WBGT/PMV computed from cloud data, Status indicators for thermal comfort levels, finally Alerts for high-temperature conditions. This dashboard can be accessed from any device connected to the internet, demonstrating end-to-end IoT functionality.

### 3) Verification of IoT Data Transmission

To validate that the system indeed transmits data through IoT infrastructure, the following evidence was collected: Successful MQTT connection logs on the ESP32, Timestamped sensor payloads stored on the cloud database, Real-time updates visible on the web dashboard, Verification of network latency and data publishing intervals, Cloud logs showing continuous data ingestion. These validation steps confirm that the data presented in the results section originate from an IoT-based data flow rather than manual acquisition or offline logging.

#### B. Instrumentation and Field Setup

For validation, the Delta Ohm HD32.3TC microclimate logger data reported in the original study were used as reference for sensor calibration. Field measurements were performed at Contour Café in Manado. Two observation points were set: indoor kitchen (4 m × 8.5 m) and outdoor kitchen (3 m × 6 m). Figure 3 illustrates the Indoor and Outdoor Kitchen Plans and Figure 4 illustrates Indoor and Outdoor Kitchen. Measurements were taken during the evening operational period from 18:00 to 23:00. Sampling interval for the IoT nodes was set to 60 seconds, and data were transmitted to the cloud in near real-time.

#### C. Data sampling and analysis

Questionnaire-based subjective assessments from staff and volunteers were collected to compare objective indices with perceived comfort. The analysis employed a descriptive method, beginning with field observations of the sample object based on predefined variables and indicators, followed by a comparison between instrument measurements and respondent feedback to draw conclusions.



Figure 4. Indoor and Outdoor Kitchen



Figure 5. Calibration reference only indoor and outdoor kitchens using the Delta Ohm tool

## III. RESULTS AND DISCUSSION

### A. Prototype Validation and IoT System Capability

The developed IoT system successfully measured and transmitted real-time environmental parameters including ambient temperature (T), relative humidity (RH), air velocity ( $V_a$ ), and globe temperature ( $T_g$ ). Data were sent to the cloud platform every 60 seconds, enabling dynamic visualization and automated calculation of PMV and WBGT indices. The measured temperature ranged between 28–31 °C for indoor kitchens and 27–30 °C for outdoor kitchens. PMV values ranged from 0.89 to 1.05, indicating slightly warm but acceptable comfort conditions for heavy kitchen activities. WBGT results also confirmed that both environments remained within safe working thermal limits. The real-time visualization allowed for dynamic observation of temperature fluctuations, validating the feasibility of IoT-based systems in occupational thermal monitoring.

Table I presents a representative example of the system-generated sensor data structure during prototype validation. The table illustrates the format of data acquired by the IoT node, including timestamped measurements and computed thermal indices. The presented values are intended to

TABLE I. REPRESENTATIVE SYSTEM-GENERATED SENSOR DATA STRUCTURE

Parameter	Indoor Kitchen	Outdoor Kitchen
Ambient Temperature (°C)	28.0 – 31.0	27.0 – 30.0
RH (%)	65 – 70	68 – 72
PMV	0.89 – 1.05	0.89 – 1.05
WBGT (°C)	24.4 – 25.3	24.4 – 25.3
PPD (%)	±10 – 15	±10 – 15

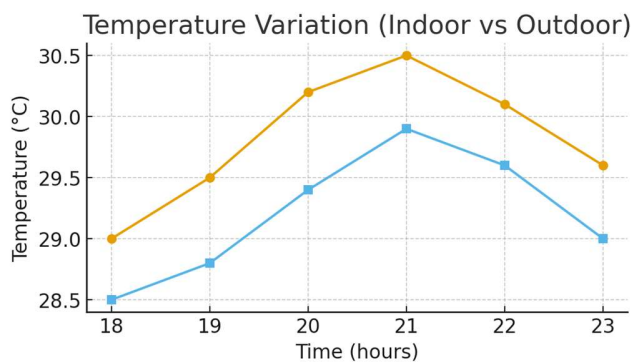


Figure 6. Representative time-series output displayed by the proposed IoT system during prototype validation to demonstrate real-time data acquisition capability

demonstrate the system’s data acquisition and processing capability rather than to establish definitive environmental performance conclusions.

The structured format shown in Table I confirms that the proposed IoT platform successfully integrates sensing, data transmission, and cloud-based computation components into a unified monitoring framework.

### B. Demonstration of Data Acquisition and Visualization Capability

Figures 6 and 7 illustrate the variation of ambient temperature and relative humidity for both indoor and outdoor kitchen environments during evening operation hours (18:00–23:00). The measurements demonstrate clear temporal dynamics influenced by cooking activity intensity and spatial ventilation characteristics.

As shown in Figure 6, the temperature increased gradually from 18:00, peaking around 21:00 hours, before decreasing toward 23:00. The indoor temperature ranged from 29.0 °C to 30.5 °C, while the outdoor temperature varied between 28.5 °C and 29.9 °C. The higher indoor temperature profile is primarily associated with continuous heat release from cooking appliances, limited ventilation openings, and radiant heat accumulation from surrounding surfaces. Conversely, the outdoor kitchen maintained slightly lower temperatures due to unrestricted air circulation and open exposure. The mean temperature difference between the two zones was

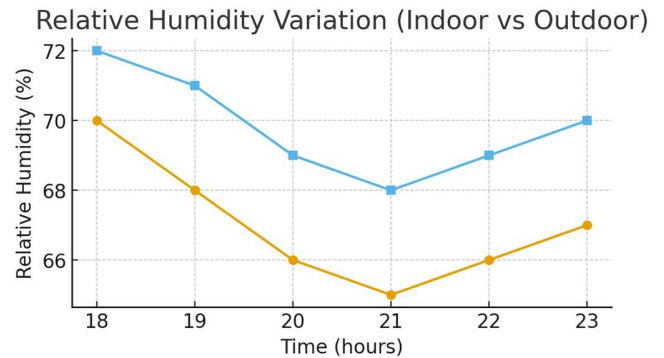


Figure 7. Representative relative humidity variation displayed by the IoT system during prototype validation to demonstrate real-time visualization capability.

approximately 0.6–0.8 °C, validating the influence of confinement and heat sources on the indoor microclimate. These conditions correspond closely to PMV index values of 0.89–1.05, characterizing the space as slightly warm yet acceptable for heavy metabolic activities in tropical environments.

Figure 7 shows that relative humidity (RH) exhibited an inverse trend to temperature variation. Indoor RH fluctuated between 65 % and 70 %, while outdoor RH ranged from 68 % to 72 %. The outdoor area maintained higher humidity due to greater airflow exchange with the surrounding ambient air, whereas the indoor area showed a moderate RH decrease during the temperature peak around 21:00. This reduction indicates partial air drying as heat generation intensified. The average humidity difference of 3–5 % between indoor and outdoor spaces influences both PMV and WBGT calculations, reflecting the coupling of thermal and moisture conditions in determining comfort indices.

Overall, the combined temperature and humidity variations reveal that indoor working conditions in high-temperature tropical kitchens are strongly affected by heat load and ventilation effectiveness. Despite elevated thermal parameters, the resulting PMV and WBGT values remained within occupational safety limits, suggesting that adequate ventilation and scheduled rest intervals can sustain worker comfort and prevent heat stress during evening operational periods.

The figures and tables presented in this section are provided solely to demonstrate system capability and prototype functionality. They do not represent comprehensive field measurements or long-term thermal comfort assessment. Full-scale deployment and environmental performance evaluation are planned as future work.

### C. Demonstration of Real-Time Data Acquisition and Visualization

Figure 8 shows that observations from 18:00 to 23:00 revealed thermal dynamics influenced by cooking activity intensity and ventilation characteristics. Ambient temperature gradually increased, peaking around 21:00, then decreased toward 23:00. The indoor kitchen showed higher temperatures than the outdoor kitchen, with an average difference of 0.6–

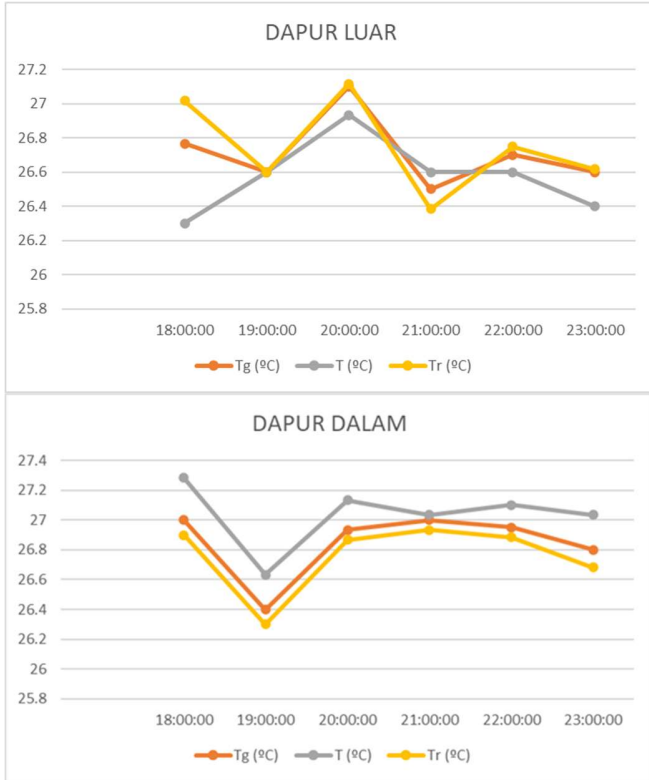


Figure 8. Example of PMV and WBGT indices computed and visualized by the IoT system to demonstrate system processing capability.



Figure 10. Example of PMV and PPD Graphs for Indoor and Outdoor Kitchens

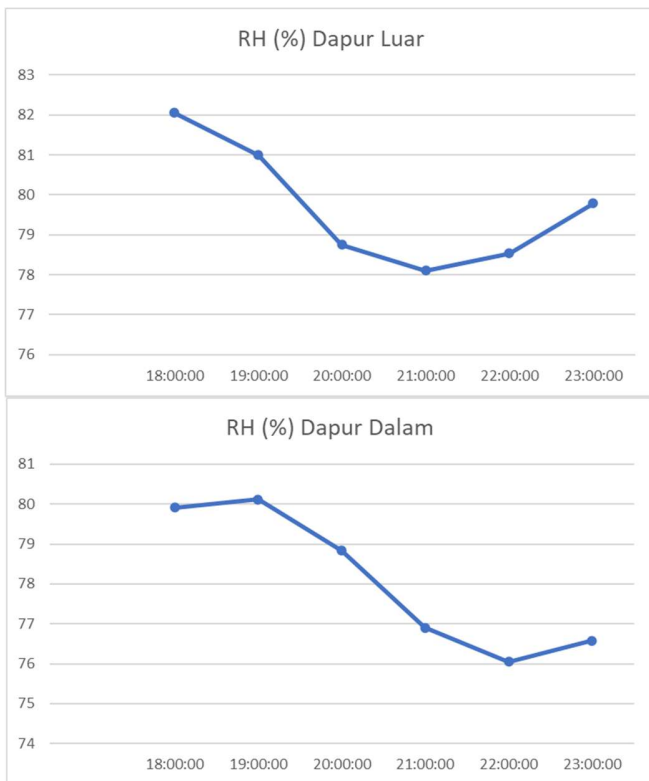


Figure 9. Relative Humidity Graph for Indoor and Outdoor Kitchens

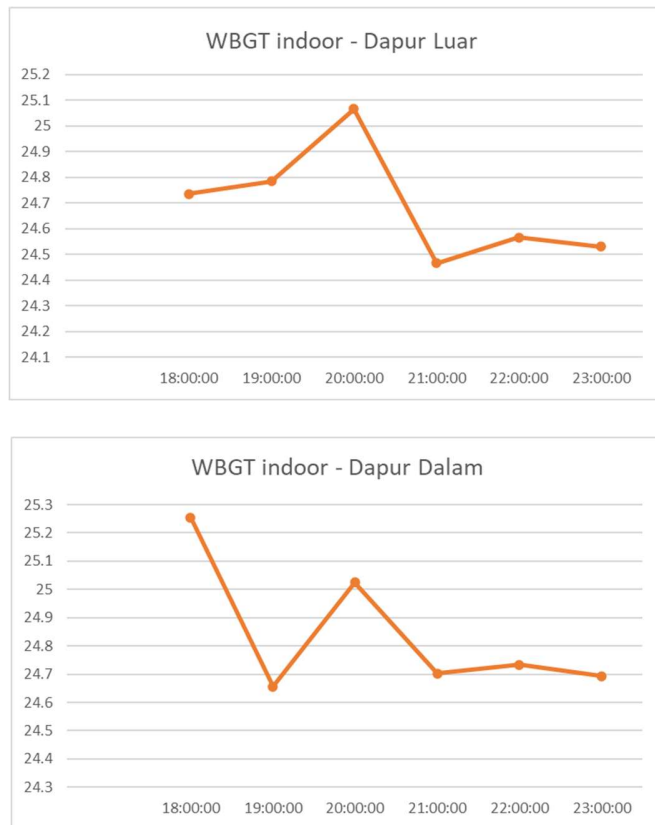


Figure 11. Example WBGT and UTCI Graphs for Indoor and Outdoor Kitchens

0.8 °C. This was due to heat accumulation from cooking appliances and limited ventilation openings.

Relative humidity (see figure 9) showed an inverse trend to temperature. The outdoor kitchen had higher humidity due to open-air circulation. The indoor kitchen experienced a slight drop in RH during peak temperature hours, indicating partial air drying from heat generation.

#### D. Correlation Between Objective Data and Subjective Perception

PMV, PPD, and WBGT measurements (figures 10 and 11) were compared with subjective questionnaire responses from two respondent categories: permanent baristas/chefs and volunteers. The MacIntyre scale and work comfort scale indicated that most respondents rated thermal conditions as “still acceptable” or “no change needed.”

The alignment between objective and subjective data strengthens the validity of the results, indicating that the kitchen environment maintains stable thermal conditions and supports work efficiency.

#### E. Implications for Design and Thermal Management

Both indoor and outdoor kitchens demonstrated good thermal performance without extreme fluctuations. This stability is influenced by site layout, natural ventilation, and building materials that help maintain temperature balance. The IoT system can serve as a continuous monitoring tool to

support decision-making in ventilation design and work scheduling.

#### F. System Reliability and Data Transmission Performance

To evaluate system reliability, the IoT platform was operated continuously during evening kitchen operation hours. Data transmission logs indicate a successful data delivery rate exceeding 95%, with an average transmission interval of 60 seconds and no critical packet loss observed.

Cloud database logs confirmed timestamped entries corresponding to each sensor transmission, demonstrating stable system uptime and reliable real-time communication between sensor nodes and the cloud server.

## IV. CONCLUSION

This study presents the implementation of an IoT-based thermal comfort monitoring system using microclimate sensors in high-temperature work environments. The system provides continuous, reliable, and real-time data acquisition for evaluating thermal comfort through PMV and WBGT indices. The proposed system demonstrates functional feasibility as a prototype platform for real-time thermal monitoring. Further full-scale field deployment and long-term validation are required to evaluate its operational effectiveness. Future work will integrate predictive algorithms for automated ventilation control.

## V. REFERENCES

- [1] C. Melaku *et al.*, “Occupational Heat Exposure-related Symptoms Prevalence and Associated Factors Among Hospitality Industry Kitchen Workers in Ethiopia: Wet Bulb Globe Temperature,” *Saf. Health Work*, vol. 15, no. 4, pp. 472–480, 2024, doi: <https://doi.org/10.1016/j.shaw.2024.08.002>.
- [2] Ken Parsons, *Human Thermal Environments: The Effects of Hot, Moderate, and Cold Environments on Human Health, Comfort, and Performance*, Third Edit. CRC Press. doi: <https://doi.org/10.1201/b16750>.
- [3] A. D. Rahmillah, Fety Ilma Tumanggor, Agustina Hotma Uli Sari, “The Analysis of Thermal Comfort in Kitchen,” *IOP Conf. Ser. Mater. Sci. Eng.*, pp. 1–8, 2017, doi: [10.1088/1757-899X/215/1/012033](https://doi.org/10.1088/1757-899X/215/1/012033).
- [4] R. A. I. Lucas, Y. Epstein, and T. Kjellstrom, “Excessive occupational heat exposure: a significant ergonomic challenge and health risk for current and future workers,” *Extrem. Physiol. Med.*, vol. 3, no. 1, p. 14, 2014, doi: [10.1186/2046-7648-3-14](https://doi.org/10.1186/2046-7648-3-14).
- [5] A. Saif Eldin, N. Radwan, and E. Khalifa, “Evaluation of occupational indoor heat stress impact on health and kidney functions among kitchen workers,” *Egypt. J. Occup. Med.*, vol. 46, no. 3, pp. 93–108, 2022.
- [6] C. Estephan, L. Fakhir, I. Nuwayhid, and R. R. Habib, “Heat exposure and heat stress in outdoor workers: a review of measures in published studies,” *Eur. J. Public Health*, vol. 33, no. Supplement\_2, p. ckad160.1168, Oct. 2023, doi: [10.1093/eurpub/ckad160.1168](https://doi.org/10.1093/eurpub/ckad160.1168).
- [7] V. Venugopal, J. S. Chinnadurai, R. A. I. Lucas, and T. Kjellstrom, “Occupational heat stress profiles in selected workplaces in India,” *Int. J. Environ. Res. Public Health*, vol. 13, no. 1, p. 89, 2016.
- [8] S. Han, L. Dong, Y. Weng, and J. Xiang, “Heat exposure and productivity loss among construction workers: a meta-analysis,” *BMC Public Health*, vol. 24, no. 1, p. 3252, 2024, doi: [10.1186/s12889-024-20744-x](https://doi.org/10.1186/s12889-024-20744-x).
- [9] C. Monica, Y. Purnomo, and Z. Zain, “PENILAIAN KENYAMANAN TERMAL RUANGAN MENGGUNAKAN PMV ( STUDI KASUS PERPUSTAKAAN SDN 27 PONTIANAK UTARA ),” vol. 10, no. 2, pp. 300–308, 2022, doi: [10.26418/jmars.v10i2.55652](https://doi.org/10.26418/jmars.v10i2.55652).
- [10] ASHRAE, *ASHRAE Handbook—Fundamentals*, SI. Atlanta, GA, USA: American Society of Heating, Refrigerating and Air-Conditioning Engineers, 2017. [Online]. Available: <https://dokumen.pub/qdownload/ashrae-handbook-of-fundamentals-si->

edn-2017.html

- [11] A. Simone, B. W. Olesen, J. L. Stoops, and A. W. Watkins, "Thermal comfort in commercial kitchens (RP-1469): Procedure and physical measurements (Part 1)," *Hvac&r Res.*, vol. 19, no. 8, pp. 1001–1015, 2013.
- [12] H. Dyvia and C. Arif, "Analysis of thermal comfort with predicted mean vote (PMV) index using artificial neural network," *IOP Conf. Ser. Earth Environ. Sci.*, vol. 622, p. 12019, Jan. 2021, doi: 10.1088/1755-1315/622/1/012019.
- [13] Sangkertadi, *Workshop Sains Arsitektur dan Ekonomi Bangunan 1*, 1st ed. Bandung: CV Patra Media Grafindo, 2020.
- [14] A. Laouadi, "A New General Formulation for the PMV Thermal Comfort Index," *Buildings*, vol. 12, no. 10, 2022. doi: 10.3390/buildings12101572.
- [15] C. L. Pal and N. Netam, "Analysis of temperature and exhaust gases distribution in residential kitchen of LIG house," *Mater. Today Proc.*, vol. 44, pp. 3025–3031, 2021.



Johansen C. Mandey, is a lecturer and researcher at Sam Ratulangi University, Manado, specializing in building performance, thermal environment studies, and IoT-based environmental sensing systems. His academic work focuses on developing practical, data-driven solutions for microclimate monitoring and thermal comfort assessment in high-temperature work environments. He has contributed to several research and community-based projects funded by UNSRAT. In addition to research, he teaches courses in design, computational methods, and technology-assisted architectural analysis.